*Progress In Electromagnetics Research B, Vol. 39, 281–299, 2012*

# ELECTROMAGNETIC VECTOR-SENSOR ARRAY PROCESSING FOR DISTRIBUTED SOURCE LOCALIZATION

**X. M. Shi*** **and Z. W. Liu**

School of Information and Electronics, Beijing Institute of Technology, Beijing 100081, China

**Abstract**—We consider the problem of direction-of-arrival (DOA) estimation for distributed signals with electromagnetic vector sensors, of which each provides measurements of the complete electric and magnetic fields induced by electromagnetic (EM) signals. In this paper, we consider situations where the sources are distributed not only in space with a deterministic angular signal density, but also in polarization with partially polarized components. A distributed signals general model with electromagnetic vector-sensor array (EMVS-DIS) is established with some reasonable assumptions. Based on the EMVS-DIS model, the minimum-variance distortionless response (MVDR) estimators for distributed source DOA are derived. MVDR estimators do not require the knowledge of the effective dimension of the pseudosignal subspace. We compare our method with the distributed signal MUSIC-like estimator in electromagnetic vector-sensor arrays. The simulation studies show significant advantages in using the proposed EMVS-DIS model with electromagnetic vector sensors. Simulation results show that the new MVDR method outperforms the MUSIC-like algorithm by reducing the estimation RMSE and improving resolution performance for scenario with distributed sources. A robustness study of MVDR localizer was also conducted via simulations.

## 1. INTRODUCTION

In most applications of array signal processing, it is usually assumed that the signals of interest are generated by far-field point sources, which means that the source energy is concentrated at discrete point.

*Received 3 February 2012, Accepted 12 March 2012, Scheduled 22 March 2012*

* Corresponding author: Xiu Min Shi (sxm@bit.edu.cn).

Based on this assumption, several high resolution direction finding methods have been proposed to estimate the source DOA, such as MUSIC [1], ESPRIT [2–5], Maximum likelihood methods [6, 37], Capon algorithm [7] and NSF [8] estimator.

Many practical scenarios can be found where the point source assumption does not hold. For instance, in wireless communication in the Arctic environment, the transmission of radio waves often undergos ionospheric scattering, so that the signal reaching the receiver would appear to form a distributed source. In the case of low-grazing-angle propagation in maritime environment and under the situation of passive estimation of source directions of arrival, signal arrives at the radar receiver via both a direct and an indirect path, the latter produced by reflections on the smooth and scatter of rough sea surface [9]. In wireless communications, due to local scattering in the vicinity of the mobile, the source is no longer viewed by the array as a point source as it represents a spatially distributed source with some central angle and angular spread [10]. Thus, the application of the conventional point sources high resolution DOA estimation methods to such problems mentioned above will show grave deterioration in performance [11].

Distributed source models have been frequently investigated in many works including [9–13]. Valaee et al. firstly proposed distributed narrowband sources model with scalar-sensor array in [12], then developed a high-resolution technique for localization, which is distributed source parameter estimator (DSPE) [14]. Others proposed dispersed signal parameter estimator (DISPARE) in [15], a class of weighted subspace fitting algorithms in [16], the maximum likelihood (ML), and minimum-variance distortionless response (MVDR) estimators in [17]. These methods gave consistent parameter estimates, but all based on scalar-sensor array, so they can not make use of all available electric and magnetic information of the source.

Nehorai and Paldi firstly proposed vector-sensor array which consists of six spatially colocated but diversely polarized antennas, separately measuring all three electrical-field components and all three magnetic-field components of the incident electromagnetic waves [18, 19]. They have also developed direction for finding algorithms exploiting all six electromagnetic components [19], which show significant advantages in using the proposed Electromagnetic Vector Sensors (EMVS). Wong and Zoltowski [20] and Li [21] separately proposed DOA estimator with EMVS. These estimators are assumed far-field point sources.

The present paper investigates both coherently distributed (CD)

and incoherently distributed (ID) sources using EMVS. We can find two types of distributed sources, i.e., CD and ID sources [14]. The CD source means that the signal components arriving from different continuum directions can be modeled as the delayed and proportioned replicas of the same signal [14]. On the other hand, all signals coming from different directions are totally uncorrelated for ID sources. In this paper, we propose a distributed signals general model with Electromagnetic Vector Sensors (EMVS-DIS). To the best of the authors' knowledge, this is the first time that distributed sources parameters estimation has been considered in both spatial and polarization field distributions with Electromagnetic Vector array. In this new model, both spatial field and polarization field distribution have been taken account in. We also proposed the minimum-variance distortionless response (MVDR) estimators for CD and ID source, respectively.

The paper is organized as follows. In the following section, we formulate the problem and propose the EMVS-DIS model. In Section 3, we develop the MVDR parameter estimation technique for the distributed sources with EMVS. The computer simulations are presented in Section 4. Section 5 summarizes our findings.

## 2. PROBLEM FORMULATION AND MODELING

The unit vector $r_k$ is pointed from the origin in Cartesian coordinates toward the source, as depicted in Figure 1. $r_k$ can be expressed as follows:

$$r_k = \begin{bmatrix} u_k \\ v_k \\ w_k \end{bmatrix} = \begin{bmatrix} \sin\theta_k \cos\varphi_k \\ \sin\theta_k \sin\varphi_k \\ \cos\theta_k \end{bmatrix} \tag{1}$$

where $0 \leq \theta_k < \pi$ denotes the signal's elevation angle; $0 \leq \varphi_k < 2\pi$ symbolizes the azimuth angle.

### 2.1. Point Sources Model

Uncorrelated transverse electromagnetic plane waves impinge upon a three-dimensional (3-D) array of identically oriented $L$ elements electromagnetic vector-sensors. The $L$ elements along the $y$-axis with $d$ (half wave length) inter-element spacing were chosen (see Figure 2). Every sensor consists of six spatially colocated but diversely polarized antennas, namely, three electric and three magnetic orthogonal sensors (dipoles and loops).

The complex envelope of the array output has three electric-field vectors, and three magnetic-field vectors may expressed in Cartesian

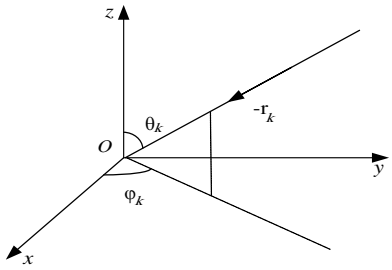


**Figure 1.** The unit vector $r_k$.

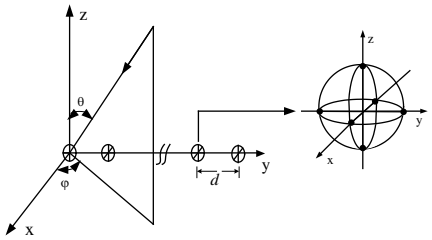


**Figure 2.** Electromagnetic vector sensors array.

coordinates as

$$\mathbf{x}(t)=[x_1(t),x_2(t)\ldots x_{6L}(t)]^T=\sum_{k=1}^{M}\mathbf{a}^{(L)}(\theta_k,\varphi_k,\gamma_k,\eta_k)s_k(t)+n(t) \quad (2)$$

where $M$ is the number of cochannel signals, and $\mathbf{a}^{(L)}(\theta_k, \varphi_k, \gamma_k, \eta_k)$ is the array manifold for the entire $L$-elements electromagnetic vector-sensor array.

$$\mathbf{a}^{(L)}(\theta_k,\varphi_k,\gamma_k,\eta_k)\overset{\text{def}}{=}\mathbf{a}(\theta_k,\varphi_k,\gamma_k,\eta_k)\otimes\underbrace{\begin{bmatrix}q_1(\theta_k,\varphi_k)\\ \vdots \\ q_L(\theta_k,\varphi_k)\end{bmatrix}}_{\overset{\text{def}}{=}\mathbf{q}(\theta_k,\varphi_k)} \quad (3)$$

where $\otimes$ symbolizes the Kronecker-product operator. $\mathbf{q}(\theta_k, \varphi_k)$ is inter electromagnetic vector-sensor array spatial phase factor. The $k$-th narrow-band point source to the $l$-th electromagnetic vector sensor at the location $(x_l, y_l, z_l)$ is

$$q_l(\theta_k,\varphi_k)=e^{j2\pi((x_lu_k+y_lv_k+z_lw_k)/\lambda)} \quad (4)$$

$\mathbf{a}(\theta_k, \varphi_k, \gamma_k, \eta_k)$ is the spatial response in matrix notation of the single electromagnetic vector sensor.

$$\mathbf{a}(\theta_k,\varphi_k,\gamma_k,\eta_k)=\underbrace{\begin{bmatrix}\cos\varphi_k\cos\theta_k & -\sin\varphi_k\\ \sin\varphi_k\cos\theta_k & \cos\varphi_k\\ -\sin\theta_k & 0\\ -\sin\varphi_k & -\cos\varphi_k\cos\theta_k\\ \cos\varphi_k & -\sin\varphi_k\cos\theta_k\\ 0 & \sin\theta_k\end{bmatrix}}_{\overset{\text{def}}{=}\mathbf{V}(\theta_k,\varphi_k)}\underbrace{\begin{bmatrix}\sin\gamma_k e^{j\eta_k}\\ \cos\gamma_k\end{bmatrix}}_{\overset{\text{def}}{=}P(\gamma_k,\eta_k)} \quad (5)$$

where $0 \leq \gamma_k < \pi/2$ represents the auxiliary polarization angle; $0 \leq \eta_k < 2\pi$ signifies the polarization phase difference.

Note that $\mathbf{V}(\theta_k, \varphi_k)$ depend only on the sources' spatial angular locations, and $P(\gamma_k, \eta_k)$ depend only on the incident signals' polarization states.

Equation (2) may be written in matrix notation as

$$\mathbf{x}(t) = [x_1(t), x_2(t) \ldots x_{6L}(t)]^T = \mathbf{AS}(t) + \mathbf{n}(t) \tag{6}$$

where

$$\mathbf{A} = \left[\mathbf{a}^{(L)}(\theta_1,\varphi_1,\gamma_1,\eta_1),\ \mathbf{a}^{(L)}(\theta_2,\varphi_2,\gamma_2,\eta_2),\ \ldots\ \mathbf{a}^{(L)}(\theta_M,\varphi_M,\gamma_M,\eta_M)\right]$$

$$\mathbf{S}(t) = [s_1(t), s_2(t) \ldots s_M(t)]^T\ \mathbf{n}(t) = [n_1(t), n_2(t) \ldots n_{6L}(t)]^T$$

$\mathbf{n}(t)$ symbolizes the $6L \times 1$ additive complex-valued zero-mean white noise vector.

## 2.2. Models for Distributed Sources

Consider a three-dimensional array of L elements EMVS (see Figure 2) monitoring a wave of $M$ distributed narrowband sources in additive background noise. The time dispersion introduced by the multipath and diffusion propagation is assumed to be small in comparison with the reciprocal of the bandwidth of the emitted signals. Below, we discuss signal sources, respectively, distribution in spatial field and polarization field.

### *2.2.1. Spatial Field Distribution*

Firstly we only concern source spatial distribution, under deterministic polarization state assumption (We will talk about polarization state distributed property later, and then give completely distributed source model). The angular signal density of $k$-th distributed source can be denoted [14] as

$$s(\theta, \varphi; \psi_k) = s_k g(\theta, \varphi : \psi_k) \tag{7}$$

The random component $s_k$ represents the temporal behavior of the source. The deterministic complex-valued function $g(\theta, \varphi : \psi_k)$ of $\theta$ and $\varphi$ characterizes the spatial distribution of the source. $\psi_k$ is the unknown parameter vector. It is natural to assume that the incident waves deterministic angular signal density in azimuth is independent of elevation. This assumption is not only intuitive but also supported by experimental data analyzed in [22] by Taga. Taga proposed the Gaussian density function in elevation and uniform density function in azimuth and supported by experimental data.

$$g(\theta, \varphi : \psi_k) = g_{ak}(\varphi : \psi_k) * g_{ek}(\theta : \psi_k) \tag{8}$$

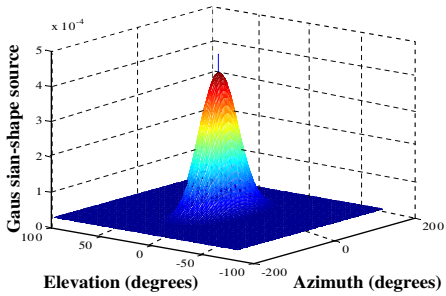


**Figure 3.** Gaussian-shape in both azimuth and elevation of distributed source.

where $g_{ak}(\varphi)$ and $g_{ek}(\theta)$ are azimuth and elevation angular signal density, respectively, and the symbol "*" represents the product operator. For example, Figure 3 depicts a Gaussian-shape in azimuth and elevation distributed source.

The complex envelope representation of the array output observation vector can be given by

$$\mathbf{x}(t)=\sum_{k=1}^{M}\int_{0}^{\pi}\iint_{0}^{2\pi}\mathbf{a}^{(L)}(\theta,\varphi,\gamma,\eta)s_k(t)g_{ak}(\varphi:\psi_k)*g_{ek}(\theta:\psi_k)d\varphi d\theta+\mathbf{n}(t) \quad (9)$$

The integral is response to the continuum components of signals in $\theta$ and $\varphi$. For simplicity, we define

$$a'(\theta,\varphi,\gamma,\eta:\psi_k)=\int_{0}^{\pi}\iint_{0}^{2\pi}\mathbf{a}^{(L)}(\theta,\varphi,\gamma,\eta)g_{ak}(\varphi:\psi_k)*g_{ek}(\theta:\psi_k)d\varphi d\theta$$

$$k=1,2,\ldots M \quad (10)$$

And let $A'(\psi)$ be the matrix of the column vectors $a'(\psi_k)$. Equation (9) may be written in matrix notation as

$$\mathbf{x}(t)=A'(\psi)\mathbf{S}(t)+\mathbf{n}(t) \quad (11)$$

where $A'(\psi)=[a'(\psi_1), a'(\psi_2), \ldots a'(\psi_M)]$; $\mathbf{S}(t)=[s_1(t), s_2(t) \ldots s_M(t)]^T$; $\mathbf{n}(t)=[n_1(t), n_2(t) \ldots n_{6L}(t)]^T$.

### *2.2.2. Polarization Field Distribution*

Polarization is a nature property of electromagnetic (EM) wave. The polarization state of EM wave is a function of time. In particular, a completely polarized wave has a constant state of polarization,

whereas a partially polarized signal varies with time. In a variety of applications, partially polarized or unpolarized signals are a general type of EM wave, and only a limited case of scenario's signal is a completely polarized EM wave. For example, as the transmitting Radar rotates itself to scan over the desired sector, the polarization of signals received at an observation point varies with time [23–28], even though the original transmitted wave is completely polarized. This variation occurs because of the nonstationary behavior of targets, clutter, rough surface, and other disturbance sources. In wireless communication in the Arctic environment, the transmission of signals is often undergone ionospheric scattering, so that the polarization of signals reaching the receiver would appear to be partially polarized [29, 30]. In maritime environments, tracking targets flying near the sea surface is a case of low-grazing-angle propagation. The polarization of signals received is partially polarized while the sea surface is disturbed and irregular [9].

Under the unknown polarization stochastic state, we decompose scattering partially polarized signal into completely polarized and unpolarized two components, to correct the situation mentioned in Section 2.2.1 that does not concern source polarization distribution deficiency. The completely polarized component relates to the direct signal, and the unpolarized component is associated with the diffuse signal component. We conduct decomposition to signal and express it as [38]

$$p_s = p_{cp}\mathbf{p}\mathbf{p}^H + p_{\text{up}}/2{*}\mathbf{I}_2 \tag{12}$$

where $p_{cp} = \sigma_S^2 = E[|s_k(t)|^2]$; $p_{\text{up}} = \sigma_u^2 = E[|U_k^H(t) * U_k(t)|]$; $U_k(t) \in C^{2X1}$.

$\mathbf{p}$ is the polarization vector defined as in (5); $U_k(t)$ denotes the horizontal and vertical components of the diffuse signal, and they are uncorrelated. The diffuse component carries no useful message, but it provides information about the source spatial position. Hence, this component accounts for "signal" in the model, instead of as part of the noise. Then, the array output can be written as

$$\mathbf{x}(t) = \sum_{k=1}^{M} \int_0^{\pi} \int_0^{2\pi} \mathbf{a}^{(L)}(\theta, \varphi, \gamma, \eta) g_{ak}(\varphi : \psi_k) * g_{ek}(\theta : \psi_k) s_k(t) d\varphi d\theta$$

$$+ \sum_{k=1}^{M} \int_0^{\pi} \int_0^{2\pi} \mathbf{V}(\theta, \varphi) \otimes \mathbf{q}(\theta, \varphi)\, g_{ak}(\varphi : \psi_k) * g_{ek}(\theta : \psi_k) U_k(t) d\varphi d\theta + \mathbf{n}(t) \tag{13}$$

For simplicity, we define

$$\mathbf{b}^{(L)}(\theta_k,\varphi_k)=\mathbf{V}(\theta,\varphi)\otimes\mathbf{q}(\theta,\varphi);$$

$$\mathbf{b}'(\theta,\varphi:\psi_k)=\int_0^{\pi}\int_0^{2\pi}\mathbf{V}(\theta,\varphi)\otimes\mathbf{q}(\theta,\varphi)\,g_{ak}(\varphi:\psi_k)*g_{ek}(\theta:\psi_k)d\varphi d\theta$$

$$k=1,2,\ldots M \tag{14}$$

where $\mathbf{b}'(\psi_k)\in C^{6LX2}$. let $B(\psi)$ be the matrix of the column vectors $a'(\psi_k)$ and $\mathbf{b}'(\psi_k)$.

$$B(\psi)=\left[a'(\psi_1),a'(\psi_2),\ldots a'(\psi_M),\mathbf{b}'(\psi_1)\ldots\mathbf{b}'(\psi_M)\right] \tag{15}$$

Equation (13) may be written in matrix notation as

$$\mathbf{x}(t)=B(\psi)\mathbf{U}(t)+\mathbf{n}(t) \tag{16}$$

where $\mathbf{U}(t)=[s_1(t),\ s_2(t)\ \ldots\ s_M(t),\ U_1^T(t),\ U_2^T(t)\ \ldots\ U_M^T(t)]^T$; $\mathbf{n}(t)=[n_1(t),\ n_2(t)\ \ldots\ n_{6L}(t)]^T$.

We assume that the signal $s_k(t)$, noise $n_k(t)$ and "signal" $U_k^T(t)$ are mutually independent distributed complex Gaussian processes with zero mean. Then, the data model (16) allows us to write the covariance matrix of the array measurements as

$$\mathbf{R}=E(\mathbf{x}\mathbf{x}^H)=\mathbf{R}_s(\psi)+\mathbf{R}_n \tag{17}$$

where $E(\cdot)$ denotes statistical expectation; superscript $H$ represents Hermitian transposition; the noise covariance matrix is $\mathbf{R}_n=\sigma_n^2\mathbf{I}$; $\sigma_n^2$ is the noise power; $\mathbf{R}_s(\psi)$ is the noise-free covariance matrix and can be given by

$$\mathbf{R}_s(\psi)=$$

$$\sum_{k=1}^{M}\sum_{l=1}^{M}\int_0^{\pi}\int_0^{2\pi}\int_0^{\pi}\int_0^{2\pi}\mathbf{a}^{(L)}(\psi_k)s_kp_{kl}\left(\theta,\varphi,\theta',\varphi':\psi_k,\psi_l\right)s_l^*\mathbf{a}^{(L)}(\psi_l)^Hd\varphi d\theta d\varphi' d\theta'+$$

$$\sum_{k=1}^{M}\sum_{l=1}^{M}\int_0^{\pi}\int_0^{2\pi}\int_0^{\pi}\int_0^{2\pi}\mathbf{b}^{(L)}(\psi_k)U_kp_{kl}\left(\theta,\varphi,\theta',\varphi':\psi_k,\psi_l\right)U_l^*\mathbf{b}^{(L)}(\psi_l)^Hd\varphi d\theta d\varphi' d\theta' \tag{18}$$

where

$$p_{kl}\left(\theta,\varphi,\theta',\varphi':\psi_k,\psi_l\right)=g_{ak}(\varphi:\psi_k)*g_{ek}(\theta:\psi_k)*g_{al}^*(\varphi':\psi_l)*g_{el}^*(\theta':\psi_l) \tag{19}$$

and "*" represents the complex conjugation. If the signals from different sources are uncorrelated, then

$$\begin{aligned}&p_{kl}\left(\theta,\varphi,\theta',\varphi':\psi_k,\psi_l\right)=p_k\left(\theta,\varphi,\theta',\varphi':\psi_k\right)\delta_{kl}\\&=g_{ak}(\varphi:\psi_k)*g_{ek}(\theta:\psi_k)*g_{ak}^*\left(\varphi':\psi_k\right)*g_{ek}^*\left(\theta':\psi_k\right)\end{aligned} \tag{20}$$

The noise-free covariance matrix is then given by

$$\begin{aligned}&\mathbf{R}_s(\psi)\\&=\sum_{k=1}^{M}\int_0^{\pi}\int_0^{2\pi}\int_0^{\pi}\int_0^{2\pi}\mathbf{a}^{(L)}(\psi_k)\,s_k p_k\left(\theta,\varphi,\theta',\varphi':\psi_k\right)s_k^*\mathbf{a}^{(L)}(\psi_k)^H d\varphi d\theta d\varphi' d\theta'\\&+\sum_{k=1}^{M}\int_0^{\pi}\int_0^{2\pi}\int_0^{\pi}\int_0^{2\pi}\mathbf{b}^{(L)}(\psi_k)U_k p_k\left(\theta,\varphi,\theta',\varphi':\psi_k\right)U_k^*\mathbf{b}^{(L)}(\psi_k)^H d\varphi d\theta d\varphi' d\theta' \quad (21)\end{aligned}$$

Below, we discuss Equation (21) in CD and ID sources, respectively.

For CD sources, the noise-free covariance matrix can be given by

$$\begin{aligned}\mathbf{R}_s(\psi) &= \sum_{k=1}^{M} a'(\theta,\varphi,\gamma,\eta:\psi_k)\sigma_s a'\left(\theta',\varphi',\gamma,\eta:\psi_k\right)^H\\&\quad+\sum_{k=1}^{M}\mathbf{b}'\left(\theta,\varphi:\psi_k\right)\sigma_u\mathbf{b}'\left(\theta',\varphi':\psi_k\right)^H \quad (22)\end{aligned}$$

For ID sources,

$$\begin{aligned}p_k\left(\theta,\varphi,\theta',\varphi':\psi_k\right)&=p_k\left(\theta,\varphi,:\psi_k\right)\delta\left(\theta-\theta'\right)\delta\left(\varphi-\varphi'\right)\\&=g_{ak}(\varphi:\psi_k)*g_{ek}(\theta:\psi_k)*g_{ak}^*(\varphi:\psi_k)*g_{eK}^*(\theta:\psi_k) \quad (23)\end{aligned}$$

Then the noise-free covariance matrix can be given by

$$\begin{aligned}\mathbf{R}_s(\psi) &= \sigma_s^2\sum_{k=1}^{M}\int_0^{\pi}\int_0^{2\pi}\mathbf{a}^{(L)}(\psi_k)p_k(\theta,\varphi:\psi_k)\,\mathbf{a}^{(L)}(\psi_k)^H d\varphi d\theta\\&\quad+\sigma_u^2\sum_{k=1}^{M}\int_0^{\pi}\int_0^{2\pi}\mathbf{b}^{(L)}(\psi_k)p_k(\theta,\varphi:\psi_k)\,\mathbf{b}^{(L)}(\psi_k)^H d\varphi d\theta \quad (24)\end{aligned}$$

## 3. MVDR LOCALIZER

By performing an eigen decomposition of correlation matrix in (17), we get

$$R = U_s\Sigma_s U_s^H + U_n\Sigma_n U_n^H \quad (25)$$

where $\Sigma_s = \text{diag}\left(\sigma_{S1}^2, \sigma_{S2}^2\ \ldots\ \sigma_{SM}^2, \sigma_{u1}^2/2, \sigma_{u1}^2/2 \ldots \sigma_{uM}^2/2, \sigma_{uM}^2/2\right)$.

$\Sigma_s$ denotes a $3M\times 3M$ diagonal matrix whose diagonal entries are the $3M$ largest eigenvalues, and $\Sigma_n$ symbolizes a $(6L-3M)\times(6L-3M)$ diagonal matrix whose diagonal entries contains the $(6L-3M)$ smallest

eigenvalues $\sigma_n^2$. Signal subspace $U_s$ is $3M$ eigenvectors $(6L \times 1)$, and $U_n$ denotes $6L \times (6L - 3M)$ matrix composed of the remaining $(6L - 3M)$ eigenvectors of correlation matrix and is the pseudo-noise subspace. $[\varphi_k, \theta_k, \gamma_k, \eta_k, \sigma_S^2, \sigma_u^2, \sigma_n^2]$ are unknown parameters, and the vector $\psi = [\varphi_k, \theta_k, \gamma_k, \eta_k]$ includes parameters of interest.

For the covariance matrix $R$ of Equation (17), the MVDR spectrum [7, 31–35] $Pu(\psi)$ is derived through the selection of the MVDR beamforming weight vector $\mathbf{w}$, which are used to control the shape of the EMVS array beam.

$$Pu(\psi) = \mathbf{w}^H \mathbf{R} \mathbf{w} \tag{26}$$

Below, we consider the MVDR spectrum of both CD and ID sources, respectively.

### 3.1. The CD Sources Localizer

For CD sources, we get weight vector $\mathbf{w}$ by solving the following linearly constrained quadratic problem.

$$\min \mathbf{w}^H \mathbf{R} \mathbf{w} \text{ subjetc to } \mathbf{w}^H \mathbf{a}'(\psi_k) = 1 \tag{27}$$

With Lagrange multiplier method, there is

$$\mathbf{w}_{opt} \mathbf{R} = \mu \mathbf{a}'(\psi_k) \tag{28}$$

So the resulting weight vector is then given by

$$\mathbf{w}_{opt} = \mu \mathbf{R}^{-1} \mathbf{a}'(\psi_k) \tag{29}$$

where

$$\mu = \frac{1}{\mathbf{a}'(\psi_k)^H \mathbf{R}^{-1} \mathbf{a}'(\psi_k)}$$

Further, the MVDR spectrum as

$$Pu(\psi) = \frac{1}{\mathbf{a}'(\psi)^H \hat{\mathbf{R}}^{-1} \mathbf{a}'(\psi)} \tag{30}$$

So the vector $\psi$ of CD sources can be estimated by locating the peaks of $Pu(\psi)$.

$$\hat{\psi} = \arg \max_{\psi} \frac{1}{\mathbf{a}'(\psi)^H \hat{\mathbf{R}}^{-1} \mathbf{a}'(\psi)} \tag{31}$$

For localization, a multi-dimensional space search step is performed to find the maxima of $Pu(\psi)$. These maxima are the estimates of the signal parameter vectors.

### 3.2. The ID Sources Localizer

For simplicity, from Equation (24) we define

$$\mathbf{p}_{ak}(\psi_k) = \int_0^{\pi}\int_0^{2\pi} \mathbf{a}^{(L)}(\psi_k) p_k(\theta,\varphi:\psi_k)\,\mathbf{a}^{(L)}(\psi_k)^H\, d\varphi d\theta \quad (32)$$

$$\mathbf{p}_{bk}(\psi_k) = \int_0^{\pi}\int_0^{2\pi} \mathbf{b}^{(L)}(\psi_k) p_k(\theta,\varphi:\psi_k)\,\mathbf{b}^{(L)}(\psi_k)^H\, d\varphi d\theta \quad (33)$$

We assume that the sources' powers are equal. Equation (24) simplifies to

$$\mathbf{R}_s(\psi) = \sigma_s \sum_{k=1}^{M} p_{ak}(\psi_k) + \sigma_u \sum_{k=1}^{M} p_{bk}(\psi_k) \quad (34)$$

For ID sources, we extend the MVDR Capon spatial filter[31] to the EMVS-DIS model as

$$\min \mathbf{w}^H \mathbf{R}\mathbf{w} \text{ subjetc to } \mathbf{w}^H \mathbf{p}(\psi_k)\,\mathbf{w} = 1 \quad (35)$$

where $\mathbf{p}(\psi_k) = \mathbf{p}_{ak}(\psi_k) + \varepsilon \mathbf{p}_{bk}(\psi_k)$, $\varepsilon$ is a ratio of diffuse components to direct components in induced signals. Equation (35) maintains distortionless spatial response to a hypothetical source's covariance matrix with the unknown vector parameter of interest, while maximally suppressing the contribution of interference sources and noise.

With Lagrange multiplier method, there is

$$\mathbf{R}\mathbf{w} = \mu p(\psi_k)\,\mathbf{w} \quad (36)$$

Multiplying Equation (36) by $\mathbf{w}^H$ from left and using the constraint of (35), we obtain that

$$\mu = \mathbf{w}^H \mathbf{R}\mathbf{w} = Pu(\psi) \quad (37)$$

Therefore, the smallest generalized eigenvalue of the matrix pencil $\{\mathbf{R}, \mathbf{P}(\psi_k)\}$ is equal to the minimal value of the objective function $Pu(\psi)$.

Then the MVDR spectrum as

$$Pu(\psi) = \lambda_{\min}(\{\mathbf{R}, \mathbf{P}(\psi_k)\}) \quad (38)$$

So the vector $\psi$ of ID sources can be estimated by locating the peaks of

$$\hat{\psi} = \arg\max_{\psi} \frac{1}{\lambda_{\max}(\{\mathbf{R}^{-1}\mathbf{P}(\psi_k)\})} \quad (39)$$

The parameter vector estimates can be obtained from the maxima of (39). Generally, a multi-dimensional search is required.

## 4. SIMULATION RESULTS

In this section, we evaluate the performance of the proposed techniques in different scenarios. We consider an EMVS array that comprises several colocated vector sensors as Figure 2, measuring all three electrical-field components and all three magnetic-field components. Each sensor is aligned with the axis $y$ of the Cartesian coordinate system with element spacing $d = \lambda/2$ ($\lambda$ is the wavelength at the operating frequency). The azimuth angular signal density of sources is assumed to be uniform.

$$g_{ak}(\varphi) = \begin{cases} \dfrac{1}{2\Delta_{1k}}, & |\varphi - \varphi_k| < \Delta_{1k} \\ 0, & \text{otherwise} \end{cases} \tag{40}$$

$\Delta_{1k}$ is the extension width of uniform density, and $\varphi_k$ is central angle of arrival. The elevation angular signal density of the sources is assumed to be Gaussian density

$$g_{ek}(\theta) = \frac{1}{\sqrt{2\pi}\Delta_{2k}} \exp\left(-\frac{(\theta - \theta_k)^2}{2\Delta_{2k}^2}\right) \tag{41}$$

where $\theta_k$ and $\Delta_{2k}$ are the central angle of arrival and the extension width of Gaussian density, respectively.

In our simulation, the additive white noise is, zero mean, complex Gaussian. SNR is defined as

$$SNR = (1/M)\sum_{k=1}^{M}\left(\left[|s_k(t)|^2\right] + \left|U_k^H(t) * U_k(t)\right|\right)/\sigma_n^2 \tag{42}$$

In the first scenario, two equal power CD sources impinge upon a 2-element EMVS array, with the following parameters values:

$$\varphi_1 = 25^\circ \quad \varphi_2 = 26^\circ; \quad \theta_1 = 20^\circ \quad \theta_2 = 45^\circ;$$
$$\Delta_{11} = 0.5^\circ \quad \Delta_{21} = 1.0^\circ; \quad \Delta_{12} = 0.5^\circ \quad \Delta_{22} = 1.0^\circ.$$

The polarization states are

$$\gamma_1 = 60^\circ \quad \gamma_2 = 45^\circ; \quad \eta_1 = 45^\circ \quad \eta_2 = 90^\circ.$$

The SNR is fixed at 10 dB, and 200 independent snapshots are used to estimate the array covariance matrix. Figure 4 shows the spectrum of the proposed CD model and MVDR algorithm. We can observe that the proposed method successfully locates the two sources.

In the second scenario, three equal power ID sources impinge upon a 2-element EMVS array, with the following parameters values:

$$\varphi_1 = 45^\circ \quad \varphi_2 = 60^\circ \quad \varphi_3 = 30^\circ; \quad \theta_1 = 35^\circ \quad \theta_2 = 45^\circ \quad \theta_3 = 20^\circ;$$
$$\Delta_{11} = \Delta_{12} = \Delta_{13} = 0.5^\circ; \quad \Delta_{21} = \Delta_{22} = \Delta_{23} = 1.0^\circ.$$

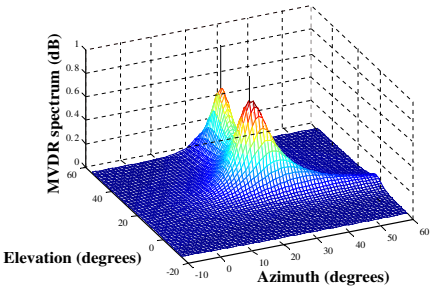


**Figure 4.** Spectrum of CD MVDR algorithm.

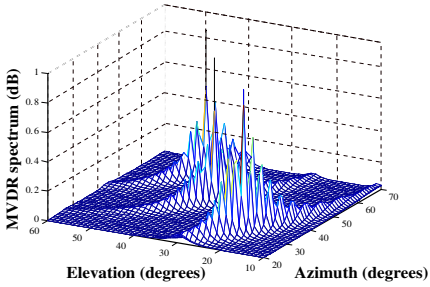


**Figure 5.** Spectrum of ID MVDR algorithm.

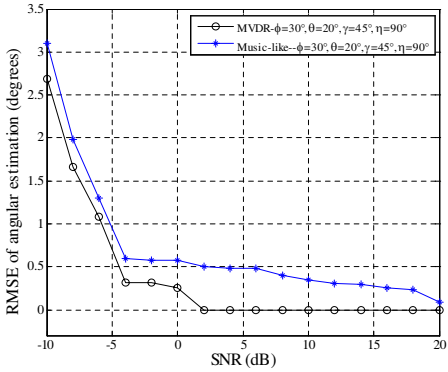


**Figure 6.** RMSE of $\varphi$ and $\theta$ versus SNR.

The polarization states are

$$\gamma_1 = 60^\circ \quad \gamma_2 = 45^\circ \quad \gamma_3 = 45^\circ; \quad \eta_1 = 45^\circ \quad \eta_2 = 90^\circ \quad \eta_3 = 30^\circ.$$

The SNR is fixed at 10 dB, and 200 independent snapshots are used to estimate the array covariance matrix. Figure 5 show the spectrum of the proposed ID model and MVDR algorithm. We can observe that the proposed method successfully locate the three sources.

In the third scenario, a CD sources impinge upon a 2-element EMVS array, with the following parameters values:

$$\varphi_1 = 30^\circ, \quad \theta_1 = 20^\circ; \quad \Delta_{11} = 0.5^\circ, \quad \Delta_{21} = 1.0^\circ;$$

The polarization states are $\gamma_1 = 45^\circ, \eta_1 = 90^\circ$.

Figure 6 shows a comparison between the performances of the MVDR and MUSIC-like [36] method for CD source. We use 200 independent snapshots to estimate the array covariance matrix. The curves in Figure 6 plot the central direction-angles' (elevation angle

and azimuth angle) composite estimation Root Mean-Square Error (RMSE) at various signal-to-noise ratio (SNR) levels, using the MVDR and MUSIC-like method. The RMSE is computed by taking square root of the mean of the respective variances of $\varphi$ and $\theta$, and the RMSE of all the following figures in this paper is similarly computed. The performances of all estimations are obtained by means of 100 independent Monte Carlo simulation experiments.

From Figure 6 one can observe that the MVDR localizer is superior to the MUSIC-like method at all SNRs, and for SNR above 2 dB estimation RMSE decreased nearly to zero.

In the next example, the robustness of MVDR to signal DOA and polarization parameters is evaluated. In this example, one CD source impinges upon a 2-element EMVS array. Figure 7 to Figure 10 plot the RMSE versus one parameter varying in different ranges, respectively. The other parameters values are the same as in the third scenario. The SNR is equal to 8 dB. Two-hundred snapshots are used in each of the 100 independent Monte Carlo simulation experiments.

From Figure 7 one can observe that the RMSE of MVDR localizer's central spatial angular estimation is under 0.05 at all azimuth angles. At approximately 90° and 270°, RMSE is greater than RMSE at other azimuth angles, though they are nearly 0.04 and 0.05 degree, respectively. This can be explained by the fact that all the array spatial phase factor $\mathbf{q}(\theta_k, \varphi_k)$'s elements is equal to 1, and one electric-field sensors and one magnetic- sensors can not obtain signal at the two direction.

Figure 8 at 0° and 90° point of elevation angle can be explained by the fact that two electric-field sensors and two magnetic-sensors cannot obtain signal.

From Figures 9 and 10, the RMSEs of the two cases as a function

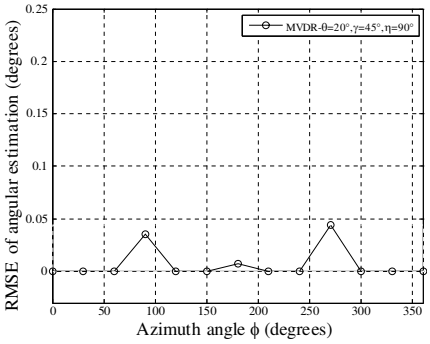


**Figure 7.** RMSE of $\varphi$ and $\theta$ versus $\varphi$.

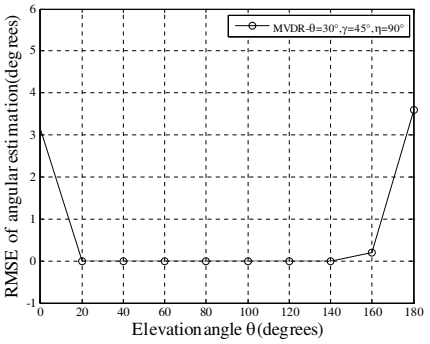


**Figure 8.** RMSE of $\varphi$ and $\theta$ versus $\theta$.

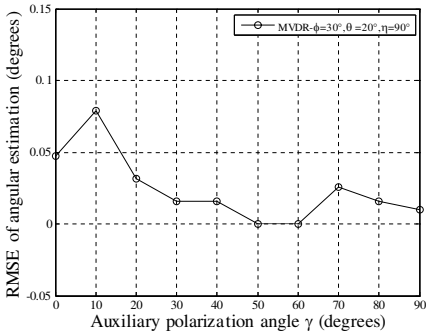


**Figure 9.** RMSE of $\varphi$ and $\theta$ versus $\gamma$.

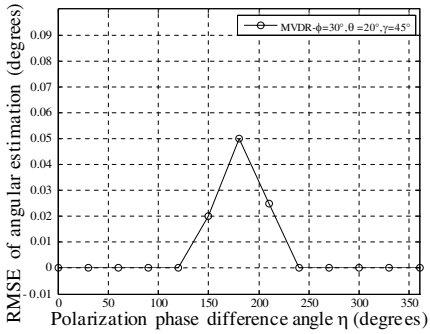


**Figure 10.** RMSE of $\varphi$ and $\theta$ versus $\eta$.

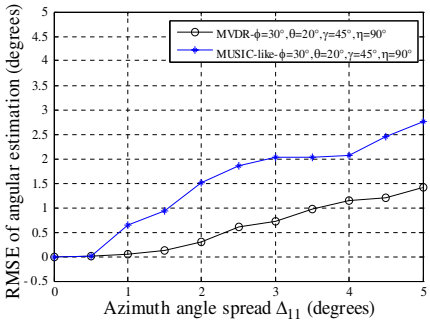


**Figure 11.** RMSE of $\varphi$ and $\theta$ versus $\Delta_{11}$.

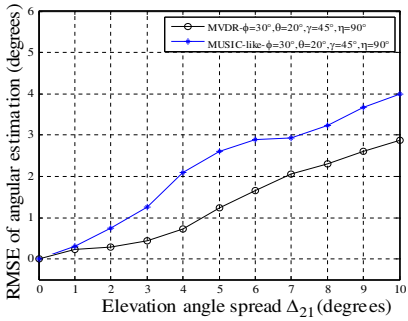


**Figure 12.** RMSE of $\varphi$ and $\theta$ versus $\Delta_{21}$.

of polarization show that the proposed MVDR localizer work well in all polarization states. MVDR method was able to resolve and estimate the DOA at all signal polarization.

In the last example, we examine the performance of the estimators when the angular spread of the source increases. Here, single ID source impinge upon a 2-element EMVS array with the following parameters values:

$$\varphi_1 = 30^\circ, \quad \theta_1 = 20^\circ; \quad \Delta_{11} = 0.5^\circ, \quad \Delta_{21} = 1.0^\circ;$$

The $\Delta_{11}$ and $\Delta_{21}$ are only for Figures 12 and 11 respectively. The polarization states are

$$\gamma_1 = 45^\circ, \quad \eta_1 = 90^\circ.$$

The SNR is equal to 8 dB. The performances of the estimators are obtained by means of 100 Monte Carlo simulations for calculating

the RMSE. The number of snapshots used to estimate the sample covariance matrix is 200.

Figures 11 and 12 show the RMS error of central spatial angular estimates versus the angular spread of azimuth and elevation angle. The two figures show a comparison between the performance of the MVDR and MUSIC-like method. We can observe that the proposed MVDR localizer is robust in the single-source case and widely separated sources situation. The proposed estimator has great advantage relative to MUSIC-like method, which do require the knowledge of the effective dimension of the pseudosignal subspace.

## 5. CONCLUSIONS

A new EMVS-DIS Model for the distributed signals source has been presented. In this model, we proposed decomposing the distributed signals into polarized and unpolarized components for its polarization state "distribution" and describing spatial distribution with deterministic angular signal density. We have presented that it is possible to significantly reduce the RMSE of the central DOA parameters estimation with EMVS-DIS Model when the full EM information is exploited using electromagnetic vector sensors. The proposed MVDR algorithm does not require the knowledge of effective dimension of the pseudosignal subspace, which is the main difficulty of the existing subspace estimators. This character is extremely important to ID source parameter estimation. Furthermore, we showed that the performance of the proposed MVDR parametric estimation algorithm is super than MUSIC-like method by simulations. The proposed estimator exploits independent polarization information as well as azimuth and elevation angle (spatial information) of the source, and it exhibits a better estimation performance.

## REFERENCES

1. Schmidt, R. O., "Multiple emitter location and signal parameter estimation," *Proceedings of International Conference of RADC Spectral Estim. Workshop*, 234–258, 1979.
2. Schmidt, R. O., "Multiple emitter location and signal parameter estimation," *IEEE Trans. on Antennas and Propag.*, Vol. 34, No. 3, 276–280, 1986.
3. Roy, R. and T. Kailath, "ESPRIT — Estimation of signal parameters via rotational invariance techniques," *IEEE Trans. Acoust. Speech, Signal Processing*, Vol. 37, No. 7, 984–995, Jul. 1989.

4. Yang, P., F. Yang, and Z.-P. Nie, "DOA estimation with sub-array divided technique and interporlated esprit algorithm on a cylindrical conformal array antenna," *Progress In Electromagnetics Research*, Vol. 103, 201–216, 2010.
5. Bencheikh, M. L. and Y. Wang, "Combined esprit-root music for DOA-DOD estimation in polarimetric bistatic MIMO radar," *Progress In Electromagnetics Research Letters*, Vol. 22, 109–117, 2011.
6. Stoica, P. and K. C. Sharman, "Maximum likelihood methods for direction-of-arrival estimation," *IEEE Trans. on Acoust. Speech, Signal Processing*, Vol. 38, No. 7, 1132–1142, Jul. 1990.
7. Capon, J. "High-resolution frequency-wave number spectrum analysis," *Proceedings of the IEEE*, Vol. 57, 1408–1418, 1969.
8. Viberg, M. and B. Ottersten, "Sensor array processing based on subspace fitting," *IEEE Trans. on Signal Processing*, Vol. 39, No. 5, 1110–1121, May 1991.
9. Hurtado, M. and A. Nehorai, "Performance analysis of passive low-grazing-angle source localization in maritime environments using vector sensors," *IEEE Trans. on Aerospace and Electronic Systems*, Vol. 43, No. 4, 780–789, Apr. 2007.
10. Kalliola, K., K. Sulonen, and H. Laitinen, "Angular power distribution and mean effective gain of mobile antenna in different propagation environments," *IEEE Trans. on Vehicular Technology*, Vol. 51, No. 5, 823–837, 2002.
11. Astely, D. and B. Ottersten, "The effects of local scattering on direction of arrival estimation with MUSIC," *IEEE Trans. on Signal Processing*, Vol. 47, No. 12, 3220–3234, Dec. 1999.
12. Valaee, S., P. Kabal, and B. Champagne, "Localization of distributed sources," *Proceedings of 14th GRETSI Symp. Signal Image Processing*, 289–292, Julan-les-Pins, France, Sep. 1993.
13. Park, G. M., H. G. Lee, and S. Y. Hong, "Doa resolution enhancement of coherent signals via spatial averaging of virtually expanded arrays," *Journal of Electromagnetic Waves and Applications*, Vol. 24, No. 1, 61–70, 2010.
14. Valaee, S., B. Champagne, and P. Kabal, "Parametric localization of distributed sources," *IEEE Trans. on Signal Processing*, Vol. 43, No. 9, 2144–2153, 1995.
15. Meng, Y., P. Stoica, and K. M.Wong, "Estimation of the directions of arrival of spatially dispersed signals in array processing," *IEE Proc. of Radar, Sonar and Navigation*, Vol. 143, No. 1, 1–9, Feb. 1996.

16. Bengtsson, M., "Antenna array processing for high rank data models," Ph.D. dissertation, Royal Institute of Technology, Stockholm, Sweden, 1999.
17. Rahamim, D. and J. Tabrikian, "Source localization using vector sensor array in a multipath environment," *IEEE Trans. on Signal Processing*, Vol. 52, No. 11, 3096–3103, 2004.
18. Nehorai, A. and E. Paldi, "Superresolution compact array radiolocation technology (SuperCART) project," *Proceedings of Asilomar Conference*, 566–572, 1991.
19. Nehorai, A. and E. Paldi, "Vector-sensor array processing for electromagnetic source localization," *IEEE Trans. on Signal Processing*, Vol. 42, No. 2, 376–398, 1994.
20. Wong, K. T. and M. D. Zoltowski, "Closed-form direction finding and polarization estimation with arbitrary spaced electromagnetic vector-sensors at unknown location," *IEEE Trans. on Antennas and Propag.*, Vol. 48, No. 5, 671–681, May 2000.
21. Li, J., "Direction and polarization estimation using arrays with small loops and short dipoles," *IEEE Trans. on Antennas and Propag.*, Vol. 41, No. 3, 379–387, Mar. 1993.
22. Taga, T., "Analysis for mean effective gain of mobile antennas in land mobile radio environments," *IEEE Trans. on Vehicular Technology*, Vol. 39, No. 5, 117–131, May 1990.
23. Skolnik, M., *Radar Handbook*, 2nd edition, McGraw-Hill, 1970.
24. Giuli, D., "Polarization diversity in radars," *Proceedings of the IEEE*, Vol. 74, No. 2, 245–269, Feb. 1986.
25. Li, J. and P. Stoica, "Efficient parameter estimation of partially polarized electromagnetic waves," *IEEE Trans. on Signal Processing*, Vol. 42, No. 11, 3114–3125, Nov. 1994.
26. Li, J. and P. Stoica, "Efficient parameter estimation of partially polarized electromagnetic waves," *Proceedings of 1994 Acoustics, Speech, and Signal Processing*, 89–92, Florida, USA, Apr. 1994.
27. Ho, K. C., K. C Tan, and B. T. G. Tan, "Estimating directions-of-arrival of completely and incompletely polarized signals with electromagnetic vector sensors," *Proceedings of ICASSP*, Vol. 5, 2900–2903, May 1996.
28. Ho, K. C., K. C. Tan, and B. T. G. Tan, "Efficient method for estimating directions-of-arrival of partially polarized signals with electromagnetic vector sensors," *IEEE Trans. on Signal Processing*, Vol. 45, No. 10, 2485–2498, Oct. 1997.
29. Eroglu, A. and J. K. Lee, "Wave propagation and dispersion characteristics for a nonreciprocal electrically gyrotropic medium,"

*Progress In Electromagnetics Research*, Vol. 62, 237–260, 2006.

30. Zhao, Z. Y. and G. Chen, "The survey of ionospheric scattering function," *PIERS Online*, Vol. 1, No. 4, 22–26, Hangzhou, China, Aug. 2005.
31. Hassanien, A., S. Shahbazpanahi, and A. B. Gershman, "A generalized capon estimator for localization of multiple spread sources," *IEEE Trans. on Signal Processing*, Vol. 52, No. 1, 280–283, 2004.
32. Wang, W., R. Wu, and J. Liang, "A novel diagonal loading method for robust adaptive beamforming," *Progress In Electromagnetics Research C*, Vol. 18, 245–255, 2011.
33. Liu, F., J. Wang, C. Y. Sun, and R. Du, "Robust MVDR beamformer for nulling level control via multi-parametric quadratic programming," *Progress In Electromagnetics Research C*, Vol. 20, 239–254, 2011.
34. Mallipeddi, R., J. P. Lie, S. G. Razul, P. N. Suganthan, and C. M. S. See, "Robust adaptive beamforming based on covariance matrix reconstruction for look direction mismatch," *Progress In Electromagnetics Research Letters*, Vol. 25, 37–46, 2011.
35. Zaharis, Z. D. and T. V. Yioultsis, "A novel adaptive beamforming technique applied on linear antenna arrays using adaptive mutated boolean PSO," *Progress In Electromagnetics Research*, Vol. 117, 165–179, 2011.
36. Shi, X. M. and Y. Y. Wang, "Parameter estimation of distributed sources with electromagnetic vector sensors," *Proceedings of ICSP*, 203–206, BeiJing, China, Oct. 2008.
37. Zhou, Q.-C., H. Gao, F. Wang, and J. Shi, "Modified DOA estimation methods with unknown source number based on projection pretransformation," *Progress In Electromagnetics Research B*, Vol. 38, 387–403, 2012.
38. Hochwald, B. and A. Nehorai, "Polarimetric modeling and parameter estimation with applications to remote sensing," *IEEE Trans. on Signal Processing*, Vol. 43, 1923–1935, Aug. 1995.